The EMBO Journal Vol. 21 No. 7 pp. 1586–1596, 2002

Levels of circumsporozoite protein in the *Plasmodium* oocyst determine sporozoite morphology

Vandana Thathy[1,2], Hisashi Fujioka[3], Soren Gantt[1], Ruth Nussenzweig[4], Victor Nussenzweig[1] and Robert Ménard[5,6]

[1]Department of Pathology, Michael Heidelberger Division of Immunology, New York University School of Medicine, New York, NY 10016, [2]Departments of Medicine and of Microbiology and Immunology, Albert Einstein College of Medicine, Bronx, NY 10461, [3]Institute of Pathology, Case Western Reserve University, Cleveland, OH 44106, [4]Department of Medical and Molecular Parasitology, New York University School of Medicine, New York, NY 10010, USA and [5]Unité de Biologie et Génétique du Paludisme, Institut Pasteur, 75724 Paris Cedex 15, France

[6]Corresponding author
e-mail: rmenard@pasteur.fr

The sporozoite stage of the *Plasmodium* parasite is formed by budding from a multinucleate oocyst in the mosquito midgut. During their life, sporozoites must infect the salivary glands of the mosquito vector and the liver of the mammalian host; both events depend on the major sporozoite surface protein, the circumsporozoite protein (CS). We previously reported that *Plasmodium berghei* oocysts in which the *CS* gene is inactivated do not form sporozoites. Here, we analyzed the ultrastructure of *P.berghei* oocyst differentiation in the wild type, recombinants that do not produce or produce reduced amounts of CS, and corresponding complemented clones. The results indicate that CS is essential for establishing polarity in the oocyst. The amounts of CS protein correlate with the extent of development of the inner membranes and associated microtubules underneath the oocyst outer membrane, which normally demarcate focal budding sites. This is a first example of a protein controlling both morphogenesis and infectivity of a parasite stage.
Keywords: budding/cell division/circumsporozoite protein/*Plasmodium berghei*/sporozoite

Introduction

Malaria transmission occurs when infective sporozoites are inoculated into a susceptible vertebrate host by a female mosquito during bloodfeeding. Sporozoites are unique amongst the invasive stages of *Plasmodium* in that they must invade one target organ in each host during their infectious process. In the mosquito, they invade the secretory cells of the salivary glands to enter the salivary ducts and, once injected into a mammalian host, they rapidly invade hepatocytes where they develop into exoerythrocytic forms.

Plasmodium sporozoites have the classical structural features of invasive stages of apicomplexan parasites. They are crescent-shaped and polarized cells. Their anterior pole contains micronemes and rhoptries, secretory organelles that discharge their contents at the anterior tip of the parasite during attachment to, and penetration of host cells. Sporozoites are formed within oocysts, which are lodged between epithelial cells and the basal lamina in the mosquito midgut. The young oocyst, surrounded by a capsule, enlarges progressively as multiple mitotic nuclear divisions occur in the absence of cytokinesis. The multinucleate oocyst is then partitioned progressively as thousands of uninucleate sporozoites bud in successive waves from the plasma membrane (Terzakis *et al*., 1967; Vanderberg and Rhodin, 1967; Vanderberg *et al*., 1967; Sinden and Strong, 1978; Aikawa, 1988).

The sporozoite is limited by a trimembranous pellicle. The outer membrane is derived from the oocyst plasma membrane, and closely apposed to it lies a double inner membrane. The two inner membranes form *de novo* underneath restricted areas of the oocyst plasma membrane at the sporozoite budding sites and progressively extend as budding proceeds (Dubremetz and Torpier, 1978). Closely underlying, and possibly connected to the inner membranes, is an asymmetrical framework of longitudinally arranged microtubules that maintain the form and rigidity of the sporozoite (Vanderberg *et al*., 1967; Aikawa, 1971; Sinden, 1978; Morrissette *et al*., 1997).

The circumsporozoite protein (CS) is the major surface protein of *Plasmodium* sporozoites (Yoshida *et al*., 1980; Aikawa *et al*., 1981; Yoshida *et al*., 1981). CS is an ~350 residue protein, most probably anchored to the sporozoite outer membrane via a glycosylphosphatidylinositol (GPI) anchor (Moran and Caras, 1994). CS is thought to have multiple important functions. Specific motifs in CS are involved in sporozoite binding to mosquito salivary glands (Sidjanski *et al*., 1997; de Lara Capurro *et al*., 2000), and in sporozoite attachment to heparan sulfate proteoglycans in the liver of the mammalian host (Cerami *et al*., 1992; Pancake *et al*., 1992; Frevert *et al*., 1993; Sinnis *et al*., 1994, 1996; Gantt *et al*., 1997; Pinzon-Ortiz *et al*., 2001). CS is probably also important for sporozoite gliding motility, a form of substrate-dependent cell locomotion characteristic of Apicomplexa. Indeed, CS is secreted at the sporozoite anterior pole, translocated along the sporozoite axis and released on the substrate at the sporozoite posterior pole (Stewart and Vanderberg, 1988). In addition, following sporozoite invasion of hepatocytes, the CS released in the host cell cytoplasm may inhibit protein synthesis by binding to ribosomes (Frevert *et al*., 1998).

Disruption of the single-copy *CS* gene in *Plasmodium berghei* revealed yet another role for CS in the parasite life cycle, as mutants were incapable of generating sporozoites (Ménard *et al*., 1997). In the present study, we used *P.berghei* clones modified at the *CS* locus and transmission electron microscopy to study the role of CS in oocyst differentiation.

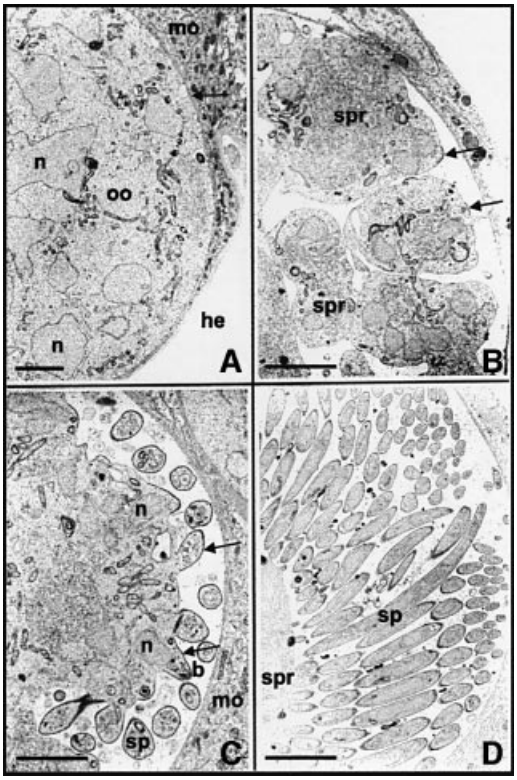

Fig. 1. Electron micrographs of oocyst development in wild-type *P.berghei*. (**A**) An early oocyst (oo) in *A.stephensi* midgut epithelium. The oocyst is limited from mosquito tissue (mo) by an electron-dense capsule (arrow), which interfaces with the hemocoel (he). Several nuclei (n) are present. (**B**) The oocyst plasma membrane then retracts from the capsule and invaginates into the oocyst cytoplasm, subdividing the oocyst into several sporoblasts (spr). Inner membranes emerge immediately beneath the plasma membrane (arrows) and demarcate sites of sporozoite budding. (**C**) As these areas evaginate (arrows), the oocyst plasma membrane and inner membranes become the trimembranous pellicle of the nascent sporozoites (b), formed anterior pole first. Nuclei (n) are seen entering sporozoite buds (b). Sporozoites that have budded off (sp) are seen in cross-section. (**D**) Eventually, the oocyst becomes packed with regularly shaped sporozoites (sp). Bars: 5 μm.

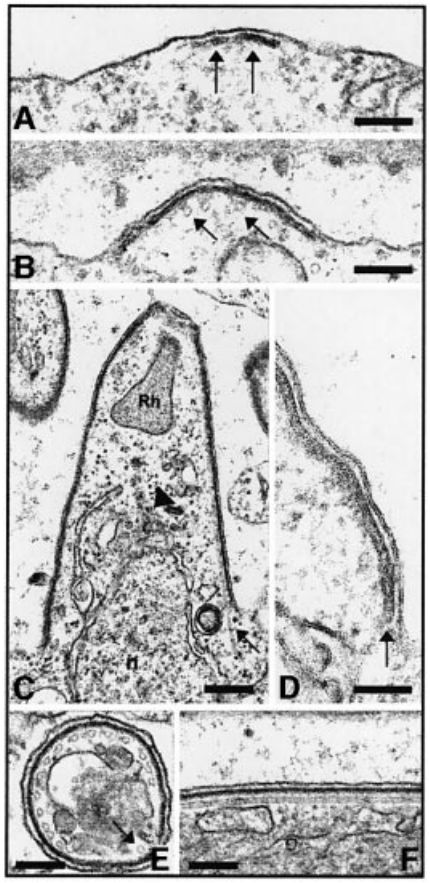

Fig. 2. Sporozoite budding in wild-type *P.berghei*. (**A**) Budding starts with the focal emergence of the inner membranes (arrows) beneath the oocyst plasma membrane. Bar: 0.5 μm. (**B**) Focal extension of the inner membranes. Subpellicular microtubules are visible in cross-section immediately below the inner membranes (arrows). Bar: 0.5 μm. (**C**) Inner membranes and microtubules (arrow) grow, shaping the nascent sporozoite. A rhoptry (Rh) is visible at the apical pole of the bud, and a nucleus (n) is seen entering the bud. Bar: 0.4 μm. (**D**) Enlarged view of the triple membrane structure of the pellicle. The closed end of the vesicle that gives rise to the two inner membranes is visible (arrow). Bar: 0.3 μm. (**E**) Cross-section of a sporozoite showing the trimembrane pellicle and the 15 subpellicular microtubules around two-thirds of the section. The arrow shows the single microtubule in the remaining third. Bar: 0.5 μm. (**F**) Longitudinal section of the sporozoite pellicle shows the plasma membrane, inner membranes and an associated microtubule. Bar: 0.5 μm.

Results

Sporozoite morphogenesis in wild-type P.berghei oocysts

Under laboratory conditions of infection, *P.berghei* oocysts are visible in mosquito midguts using phase-contrast microscopy 5 days after the infective bloodmeal. Sporozoites begin to fill these oocysts by days 10–12 post-infection. Figure 1 shows the process of sporozoite formation inside oocysts of *P.berghei* in *Anopheles stephensi* mosquitos by transmission electron microscopy. As already described (Vanderberg and Rhodin, 1967; Vanderberg *et al*., 1967), the fully grown oocyst is a spherical cell (~30–40 μm in diameter) limited by a plasma membrane and a thick capsule (Figure 1A). It contains numerous dividing nuclei and cytoplasmic membranes, including a network of flattened cisternae and circular vesicles at the periphery of the cell. Daughter cell formation starts when the plasma membrane fuses with peripheral vesicles and thus retracts from the capsule (Figure 1A). The continuing fusion with large vacuoles causes the plasma membrane to invaginate progressively into the oocyst cytoplasm, creating several cytoplasmic islands called sporoblasts (Figure 1B). Sporozoites then bud from the sporoblast periphery in successive waves (Figure 1C; see Vanderberg *et al*., 1967), and gradually fill the subcapsular space left by sporoblast retraction (Figure 1D).

Sporozoite budding is detailed in Figure 2. The first events in bud formation are the co-emergence underneath discrete areas of the oocyst plasma membrane of (i) two linear, closely aligned membranes (here referred to as inner membranes), which presumably originate in the docking and flattening of cytoplasmic vesicles at the plasma membrane (Dubremetz and Torpier, 1978); and (ii) microtubules that always closely underlie the inner membranes (Figure 2A and B; see arrows in Figure 1B). The inner membranes and microtubules then co-extend and the bud grows (Figure 2B); although the bud appears

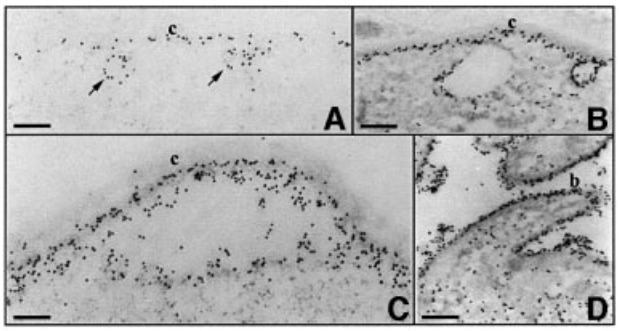

Fig. 3. Immunoelectron micrographs showing CS expression in wild-type *P.berghei* oocysts. Sections of wild-type *P.berghei* oocysts at increasing stages of development from (A) to (D) were stained with anti-CS monoclonal antibodies followed by anti-mouse IgG conjugated to 15 nm gold particles. (**A**) Gold particles are associated with the plasma membrane, which is still closely attached to the capsule (c) in the early oocyst, as well as with vesicles fusing to the plasma membrane (arrows). Bar: 0.8 μm. (**B**) CS labeling increases at the plasma membrane, while the cytoplasm remains poorly labeled. Bar: 1.5 μm. (**C**) CS labeling continues to increase as the plasma membrane retracts from the oocyst capsule. Bar: 0.8 μm. (**D**) At later stages, CS covers the surface of budding sporozoites. Bar: 1.5 μm.

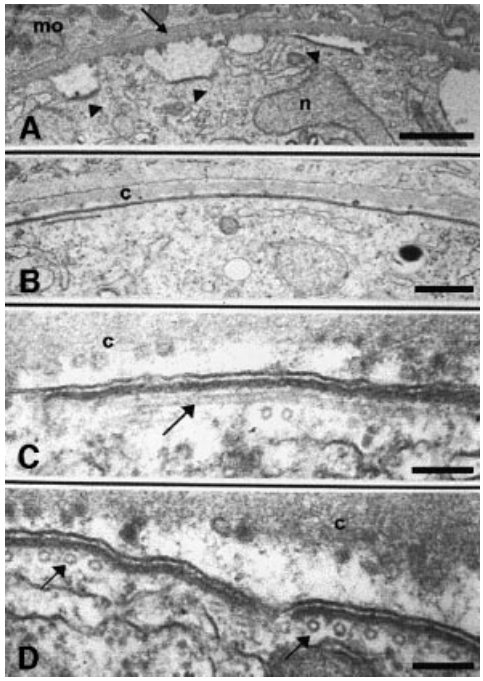

Fig. 4. Electron micrographs showing the development of CSko oocysts. Inner membranes and microtubules rapidly delineate large areas of the oocyst plasma membrane. (**A**) Extended stretches of inner membranes (arrowheads) are visible beneath the plasma membrane at early stages of plasma membrane retraction from the oocyst capsule (arrow). n, nucleus; mo, mosquito midgut tissue. Bar: 5 μm. (**B**) Continuous lining by inner membranes of an extensive area of the plasma membrane that has not retracted from the capsule (c). Bar: 2.5 μm. (**C**) The arrow shows a longitudinal section of a subpellicular microtubule. c, oocyst capsule. Bar: 0.5 μm. (**D**) Arrows show subpellicular microtubules in cross-section. Bar: 0.5 μm.

to evaginate, it may instead grow internally and be covered gradually by plasma membrane. In any event, the nascent sporozoite is limited by a continuous trimembrane pellicle, i.e. the plasma membrane and the inner membranes, and a subpellicular microtubule structure running longitudinally (Figure 2C–F). In *P.berghei*, this structure consists of 15 microtubules organized around two-thirds of the periphery of the sporozoite section and an isolated microtubule in the remaining third of the periphery (Figure 2E; see Vanderberg *et al*., 1967).

As previously shown in numerous *Plasmodium* species by immunogold labeling (Nagasawa *et al*., 1987, 1988; Posthuma *et al*., 1988; Aikawa *et al*., 1990), CS is first detected at the oocyst plasma membrane when it starts to retract from the capsule, prior to the onset of budding (Figure 3). At early developmental stages, CS is associated mainly with the plasma membrane and with vesicles that are fusing with the plasma membrane (Figure 3A and B). In contrast, only scarce amounts of CS are found in the cytoplasm or associated with cytoplasmic vesicles. Later in development, labeling increases. As the plasma membrane retracts from the capsule, CS decorates the sporoblast plasma membrane and is detectable on the capsule and in the subcapsular space (Figure 3C). When budding has started, large amounts of CS cover the entire surface of sporoblasts and sporozoites (Figure 3D).

Development of CS knockout oocysts

We previously have generated four independent *P.berghei* clones in which the wild-type *CS* gene was disrupted by homologous recombination (Ménard *et al*., 1997). These *CS* knockout (CSko) clones produced similar numbers of oocysts as wild-type *P.berghei* in *A.stephensi* midguts, but oocysts did not generate sporozoites. One of the CSko clones, CS(-)1, was examined by transmission electron microscopy (Figure 4). No difference in oocyst growth or nuclear divisions between the CSko clone and the wild-type was observed until day 10 post-infection. Nuclei were scattered randomly throughout the cytoplasm, and were surrounded by a typical nuclear envelope. Three primary differences between development of CSko and wild-type oocysts were observed. (i) In the wild-type, the inner membranes are formed only underneath a fully retracted plasma membrane (Figures 1B and 2A). In contrast, in CSko oocysts, they emerged at the early stage (~day 10 post-infection) of subcapsular vacuolization, underlying local invaginations of a plasma membrane, which was still largely in contact with the capsule (Figure 4A). (ii) While in the wild-type the emerging inner membranes are always restricted to small areas of the plasma membrane (the budding sites), in CSko oocysts they lined extensive areas of the plasma membrane, and frequently appeared to enclose the oocyst completely (Figure 4B–D). Importantly, microtubules were always associated with the aberrant inner membranes in CSko oocysts (Figure 4C and D), and the distances between individual microtubules, and between microtubules, the inner membranes and the plasma membrane were similar in wild-type and CSko oocysts (Table I). (iii) In sharp contrast to the wild type, large cytoplasmic vacuoles in CSko oocysts were frequently coated by the inner membranes, either partially (Figure 5E and F) or totally (Figure 5D and G). It is unclear, however, whether the vacuoles coated with inner membranes in CSko oocysts represented cytoplasmic vesicles on their way to the oocyst membrane, or cross-sections of deep invaginations of the oocyst plasma membrane.

Table I. Ultrastructure of the oocyst periphery in wild-type and CSko parasites

	Spacing between (nm)		
	Individual MTs (cross)	IM and OM (longitudinal)	MTs and IMC (cross and longitudinal)
Wild type	31 ± 3	12 ± 0.3	13 ± 1
CSko	32 ± 6	12 ± 0.3	13 ± 0.4

MT, microtubule; IM, inner membrane; OM, outer membrane.

Strikingly, in virtually all CSko oocysts examined, the inner membranes underneath both the plasma membrane and cytoplasmic vacuolar membranes sometimes delineated shapes that resembled sporozoites (Figure 5). These shapes grew randomly either externally (in the subcapsular space, Figure 5A and C), or internally (within vacuoles, Figure 5D–G) where areas underlined by inner membranes appeared to evaginate. Budding from the surface of CSko oocysts only occurred partially (most buds failed to pinch off) and in a direction that was parallel to the parasite syncytial mass (Figure 5A and B). This was in contrast to wild-type oocysts, in which daughter cells always bud in a direction perpendicular to the sporoblast periphery (Figures 1C, D, 2B and C). Remarkably, despite their variable and frequently anomalous shape, buds in CSko oocysts were limited by the trimembrane pellicle and subpellicular microtubules (Figure 5C), which again were separated by the same average distance as in wild-type sporozoite buds (Table I). Subsequent incorporation of cytoplasmic organelles into the developing buds apparently was not disrupted in CSko oocysts, as developing rhoptries were seen frequently at the anterior tip of buds, followed by a nucleus (Figure 5D and G).

Thus, in CSko oocysts, budding can occur but is no longer polarized and is unproductive. Inner membranes and microtubules still develop in concert but do so prematurely and extensively, and the buds that sometimes form have an abnormal shape and orientation.

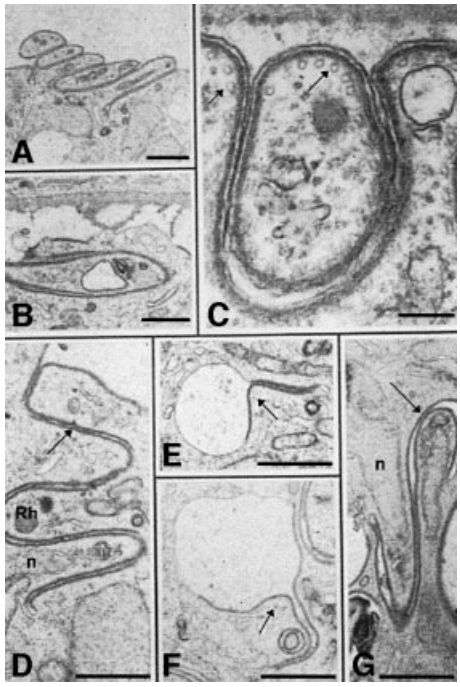

Fig. 5. Electron micrographs of CSko oocysts showing aberrant budding in the subcapsular space (A–C) and in the sporoblast cytoplasm (D–G). (**A**) Parallel stacking of bud-like structures. Bar: 3 μm. (**B**) An abnormal bud extends parallel to the sporoblast periphery instead of away into the subcapsular space. Bar: 2.5 μm. (**C**) Inner membranes and microtubules (arrows) underneath the oocyst plasma membrane and the bud outer membrane. Bar: 0.5 μm. (**D–G**) Cytoplasmic membranes lined with inner membranes (arrows), either totally (D and G) or partially (E and F). Rh, rhoptry; n, nucleus. Bars: 2.5 μm.

Genetic complementation of CS null mutants

To determine whether these features of CSko oocysts were due to the lack of CS or to an adverse effect of the disrupted locus, we introduced an intact copy of the *CS* gene into the disrupted *CS* locus of these parasites. For this, CSko erythrocytic stages, generated using a pyrimethamine-resistant dihydrofolate reductase thymidylate synthase (Pb*DHFR-TS*) gene, were transfected with plasmid pCSComp (Figure 6A). This plasmid contained the human WR99210-resistant dihydrofolate reductase (h*DHFR*) gene as a selectable marker (Fidock and Wellems, 1997; de Koning-Ward *et al*., 2000), and the wild-type *P.berghei CS* placed under the control of 1.3 kb of *CS* 5′-untranslated region (UTR) and 450 bp of *CS* 3′-UTR. Plasmid pCSComp was targeted to the disrupted *CS* locus by linearization at a unique site located 600 bp upstream of the *CS* start codon. All clones selected had the genetic structure depicted in Figure 6A and shown in Figure 6B for one representative, CSComp1. These clones had multiple copies of the plasmid integrated in tandem in the disrupted *CS* locus, or only one integrated copy along with episomal forms of the plasmid. They were thus complemented with several copies of the *CS* cassette, at least one of them being integrated at the *CS* locus.

CSComp1 parasites transmitted to *A.stephensi* mosquitos produced normal numbers of midgut sporozoites. CS production was assessed in CSComp1 sporozoites harvested from infected mosquito midguts at day 15 post-infection by western blot using anti-CS monoclonal antibodies. These sporozoites produced amounts of CS similar to wild-type sporozoites (Figure 6C). Microscopic examination indicated that the complemented sporozoites were normally shaped and displayed the typical gliding motility patterns seen in wild-type sporozoites (not shown). Sporozoites of the wild-type and complemented populations infected mosquito salivary glands to similar extents (not shown), and immunofluorescence microscopy using anti-CS antibodies confirmed normal CS expression in complemented sporozoites collected from mosquito salivary glands (Figure 6D). Salivary gland sporozoites in the two populations induced similar pre-patent periods of infection in rats after intravenous injection (not shown), and the resulting complemented erythrocytic stages were confirmed by Southern blot analysis to still contain the *CS* expression cassette(s) integrated into the disrupted *CS* locus (Figure 6B, see CSComp1-SI parasites). Therefore, reintroduction of a *CS* gene into the inactivated *CS* locus leads to normal production of CS protein and recovery of a normal sporogonic cycle. We conclude that the defective

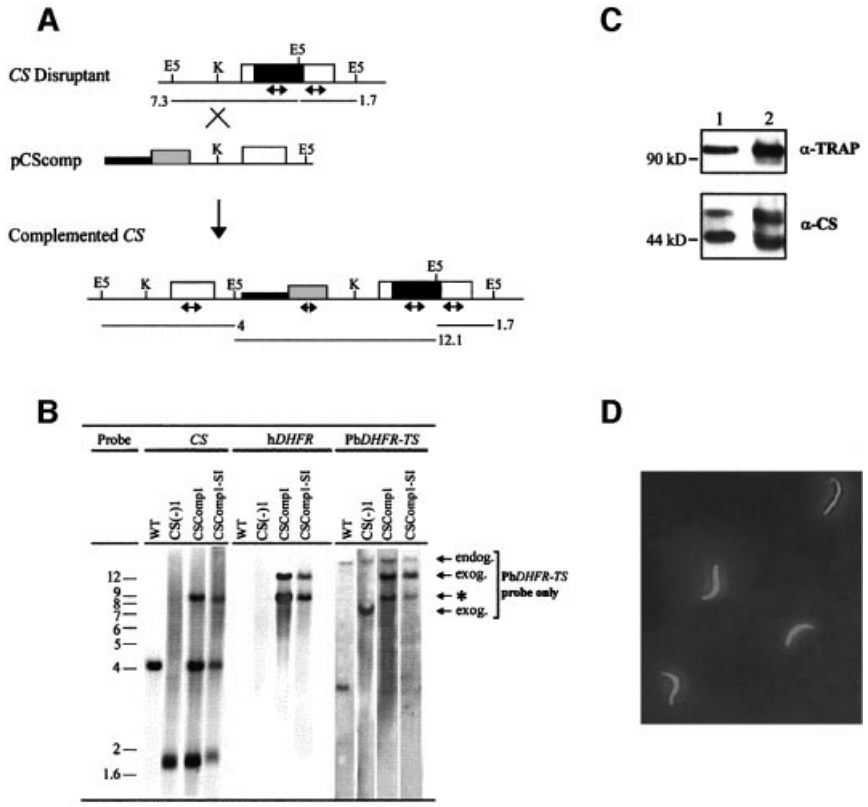

Fig. 6. Genetic complementation of the CSko clone by reintroduction of the *CS* gene into the disrupted *CS* locus. (**A**) Gene targeting at the *CS* knockout locus (*CS* disruptant) using the insertion plasmid pCSComp linearized at the unique *Kpn*I site (K) prior to transfection. The complemented *CS* locus expected to result from plasmid integration is shown below. The predicted sizes (in kb) of restriction fragments generated upon digestion of parasite genomic DNA with *Eco*RV (E5) in the *CS* knockout or the complemented *CS* locus are shown. Open boxes, *CS* coding sequences; black boxes, pyrimethamine resistance *P.berghei DHFR-TS* selection cassette; gray boxes, human *DHFR* (h*DHFR*) selection cassette; thin lines, 5′- and 3′-UTRs of *CS*; thick lines, pUC19 vector sequences; double-headed arrows, internal probes from *CS*, *P.berghei DHFR-TS* or h*DHFR* coding sequences used in Southern hybridization. (**B**) Southern blot hybridization of *Eco*RV-digested genomic DNA of wild-type *P.berghei* (WT), CSko [CS(-)1], complemented *CS* (CSComp1) and blood stages resulting from a sporozoite-induced infection by CSComp1 sporozoites (CSComp1-SI). The same blot was probed successively with *CS*, h*DHFR* and Pb*DHFR-TS* probes. Endog., endogenous Pb*DHFR-TS* gene; exog., exogenous Pb*DHFR-TS* copies originating from the *CS* knockout locus (7.3 kb) and from the complemented *CS* locus (12.1 kb); *, cross-reaction of the Pb*DHFR-TS* probe with sequences in pCSComp. (**C**) Western blot analysis of midgut sporozoite extracts from wild-type (lane 1) and complemented (CSComp1, lane 2) parasites. Sporozoites were collected from oocysts in mosquito midguts dissected at day 15 post-infection. Crude extracts from ~5 × 10^3 sporozoites from each population resolved by SDS–PAGE and transferred to a membrane were probed with anti-TRAP polyclonal antibodies (α-TRAP) and anti-CS monoclonal antibodies (α-CS). (**D**) Indirect immunofluorescence assay of CSComp1 sporozoites collected from the salivary glands of infected mosquitos dissected at day 18 post-infection. Sporozoites were permeabilized and stained using FITC-conjugated, anti-CS monoclonal antibodies.

phenotype of CSko parasites is due specifically to the lack of CS.

Construction of PINA270 clones producing low amounts of CS

To analyze further the role of CS in controlling development of the inner membranes and underlying microtubules, we constructed *P.berghei* clones that produced reduced amounts of CS by altering the 3′-UTR of *CS*. Cloning and sequencing of *CS* transcripts in *P.berghei* sporozoites have revealed numerous 3′ ends (Ruvolo *et al*., 1993). Unlike most eukaryotic messages, which are cleaved at a single site and subsequently polyadenylated, the 3′ ends of the *CS* transcripts are heterogeneous, located between nucleotides 88 and 337 after the *CS* stop codon (Figure 7A). The majority of the *CS* 3′ ends are clustered ~300 bp past the stop codon, just upstream of a 16 bp GU-rich element (Ruvolo *et al*., 1993).

We generated two *P.berghei* clones (PINA270-1 and PINA270-2) in which the *CS* gene was followed by 270 bp of its 3′-UTR. These clones were obtained in independent transformation experiments by homologous integration at the *CS* locus in wild-type *P.berghei* of insertion plasmid pPINA270 (Figure 7A and B). The targeting sequence of the plasmid starts at nucleotide 36 of *CS* and ends 270 bp after the stop codon. Southern blot hybridization indicated that the two PINA270 clones had an identical *CS* recombinant locus (shown in Figure 7C for clone PINA270-1). This locus resulted from homologous integration of more than one copy of the insertion plasmid, as depicted in Figure 7B. Since the insertion plasmid contains a truncated *CS*, only the first chromosomal *CS* copy is full length and expressed, while downstream *CS* copies are truncated and promoterless. The correct structure of the first *CS* copy in the PINA270 locus was confirmed by PCR amplification (Figure 7F, lane 1). Cloning and sequencing of two independent PCR products confirmed that the expressed copy of *CS* had a wild-type sequence and was followed by 270 bp of its 3′-UTR.

Anopheles stephensi mosquitos were infected with each of the two PINA270 clones. Extracts from midgut sporozoites prepared at days 12–15 post-infection were

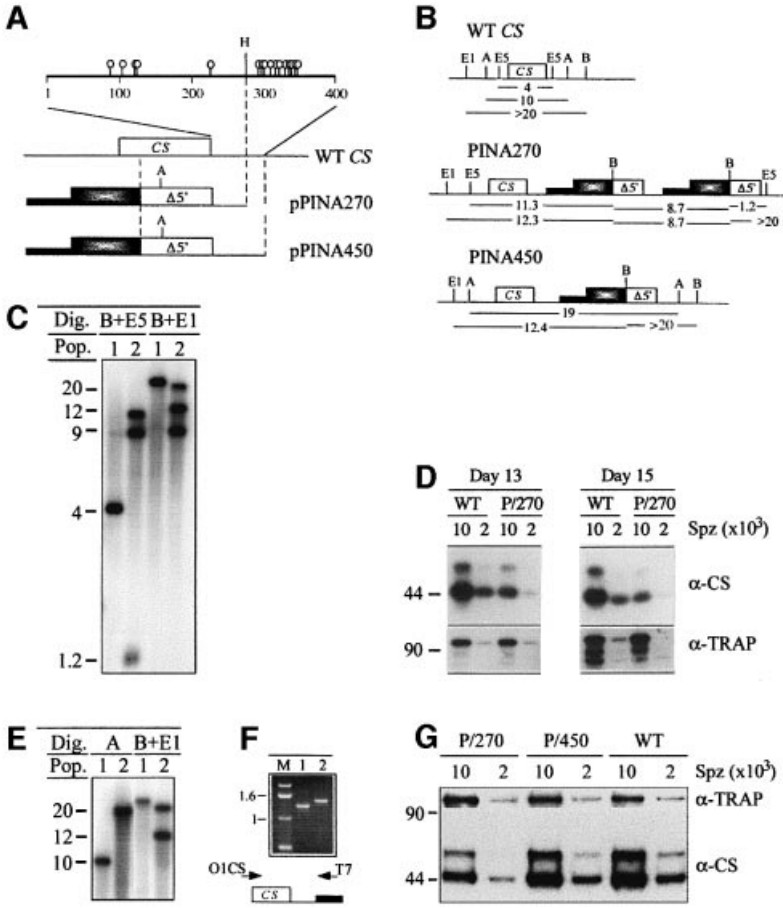

Fig. 7. Generation of PINA270 and PINA450 clones of *P.berghei* that produce low or wild-type amounts of CS, respectively. (**A**) Schematic representation of the wild-type (WT) *CS* locus and insertion plasmids pPINA270 and pPINA450, which differ only in the length of the *CS* 3′-UTR, shown enlarged above the WT *CS* locus. The lollipop symbols in the *CS* 3′-UTR show the 3′ ends of *CS* transcripts located between nucleotides 88 and 337 following the *CS* stop codon. The WT *CS* gene was targeted with plasmids pPINA270 and pPINA450, whose targeting sequences contain the distal part of the WT *CS* coding region and 270 or 450 bp of its 3′-UTR, respectively. Plasmids were linearized at a unique *Afl*II site (A) located at 250 bp from the 5′ end of the targeting sequence. Shaded boxes, *P.berghei DHFR-TS* pyrimethamine resistance cassette; thick lines, pBSKS vector sequences; H, *Hin*cII. (**B**) Structures of the WT *CS* genomic locus and the *CS* recombinant loci generated by homologous integration of plasmids pPINA270 and pPINA450. The predicted sizes (in kb) of restriction fragments generated upon digestion with *Bam*HI–*Eco*RV, *Bam*HI–*Eco*RI or *Afl*II are shown. A, *Afl*II; B, *Bam*HI; E1, *Eco*RI; E5, *Eco*RV. (**C**) Southern hybridization of WT *P.berghei* (lane 1) and the PINA270 clone (lane 2), upon digestion with *Bam*HI–*Eco*RV (lanes 1 and 2) or *Bam*HI–*Eco*RI (lanes 3 and 4) and using a *CS* probe. (**D**) Western blot analysis of midgut sporozoite extracts from the WT and PINA270 (P/270) populations. Sporozoites were harvested from oocysts in mosquito midguts at days 13 and 15 post-infection. Crude extracts separated by SDS–PAGE and transferred to a membrane were probed with anti-CS (α-CS) or anti-TRAP (α-TRAP) antibodies. (**E**) Southern hybridization of WT *P.berghei* (lane 1) and the PINA450 clone (lane 2), upon digestion with *Afl*II (lanes 1 and 2) or *Bam*HI–*Eco*RI (lanes 3 and 4) and using a *CS* probe. (**F**) PCR amplification of the expressed *CS* copy in PINA270 (lane 1) and PINA450 (lane 2) parasites using primers O1CS and T7, which anneal upstream from the region of homology and to the vector sequence, respectively. (**G**) Western blot analysis of midgut sporozoite extracts from WT, PINA270 (P/270) and PINA450 (P/450) parasites. Sporozoites were harvested from oocysts in mosquito midguts at day 15 post-infection, and analyzed as in (D).

analyzed by western blot using anti-CS antibodies. Figure 7D shows a representative experiment using wild-type and PINA270-1 midgut sporozoites collected at days 13 and 15 post-infection. Sporozoites in both PINA270 clones reproducibly contained ~5× less CS protein than wild-type sporozoites. They still produced a normal ratio of the 44 and 54 kDa forms of CS, which are thought to represent the surface molecule and intracellular precursor of CS, respectively (Yoshida *et al*., 1981). As a control, the same sporozoite extracts from wild-type and PINA270-1 sporozoites were probed with antibodies directed against thrombospondin-related anonymous protein (TRAP), another sporozoite protein (Figure 7D), and found to contain similar amounts of TRAP. Therefore, freshly produced PINA270 sporozoites (as early as day 12, the earliest time point that can be tested) produced significantly less CS protein than their wild-type counterparts.

PINA270 oocysts display intermediary levels of extension of the inner membranes and microtubules and PlNA270 sporozoites are aberrantly shaped

Sporozoite formation in the PINA270-1 clone was analyzed by transmission electron microscopy (Figure 8). At days 10–12 post-infection, ~100% wild-type oocysts displayed the normal phenotype shown in Figures 1 and 2, and all CSko oocysts displayed the phenotype described in Figures 4 and 5. At the same days post-infection, PINA270-1 oocysts displayed variable phenotypes. While a minority resembled either wild-type or CSko oocysts,

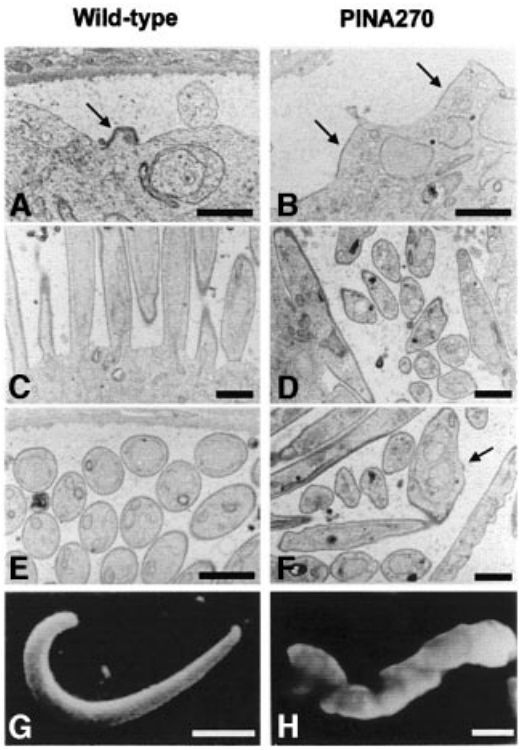

Fig. 8. Transmission electron micrographs showing sections of wild-type and PINA270 oocysts. (**A**) Focal emergence and extension of inner membranes (arrow) underneath the plasma membrane at a sporozoite bud site in a wild-type oocyst. Bar: 3 μm. (**B**) In PINA270 oocysts, inner membranes (arrows) delineate areas of the plasma membrane that are larger than in wild-type oocysts. Bar: 3 μm. (**C**) Sporozoite buds elongate perpendicular to the sporoblast periphery in wild-type oocysts. Bar: 1.5 μm. (**D**) In PINA270 oocysts, budding often occurs parallel to the sporoblast periphery. Bar: 1.5 μm. (**E**) Cross-sections of fully formed sporozoites, which are of homogenous sizes and shapes. Bar: 1.5 μm. (**F**) Longitudinal and cross-sections of sporozoites, which are of variable sizes and shapes. Note the presence of two nuclei surrounded by a single nuclear envelope in one of the sporozoites (arrow) and the 'corrugated' appearance of the sporozoite pellicles. Bar: 1.5 μm. (**G** and **H**) Scanning electron micrographs of free wild-type (G) and PINA270 (H) midgut sporozoites isolated from infected mosquitos at day 14 post-infection. Note the corrugated surface of the PINA270 sporozoite. Bars: 2 μm.

~60–70% of oocysts had intermediate features between the two types. In most PINA270-1 oocysts, the inner membranes underlined stretches of the oocyst plasma membrane that were intermediate in size between the focal sites in wild-type oocysts and the mostly uninterrupted regions in CSko oocysts (compare Figures 8A, B, and 4). The bud shapes in PINA270-1 oocysts were also intermediate between those in CSko and wild-type oocysts. Sporozoites of variable length and diameter were formed, in contrast to the evenly sized and shaped wild-type sporozoites (Figure 8E and F) and the profoundly abnormal buds in CSko oocysts (Figure 5). Frequently, in PINA270-1 oocysts, the emergence of longer areas coated by inner membranes induced the formation of wider buds than in wild-type counterparts (sometimes associated with improper segregation of nuclei into the budding daughter cells; see arrow in Figure 8F). However, similarly to the wild type, the inner membranes and the underlying microtubules were only found underneath the detached plasma membrane in PINA270-1 oocysts, and not at the stage of early subcapsular vacuolization or underneath cytoplasmic membranes, as in CSko oocysts.

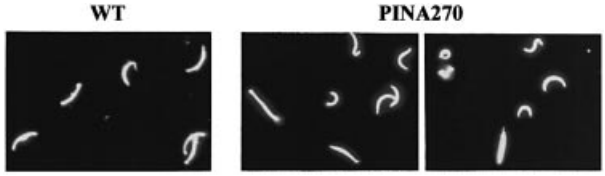

Fig. 9. Immunofluorescence labeling of wild-type and PINA270 sporozoites collected from the hemolymph of infected mosquitos at day 15 post-infection. Sporozoites were permeabilized and stained with FITC-conjugated, anti-CS monoclonal antibodies. Note the variations in size and shape of PINA270 sporozoites as compared with wild-type sporozoites.

Immunofluorescence analysis of PINA270 midgut sporozoites using anti-CS antibodies revealed that at least 50% of sporozoites in both PINA270 clones had abnormal and variable sizes and shapes, in contrast to the unchanging needle-like appearance of wild-type sporozoites (Figure 9). Approximately half of the abnormal PINA270 sporozoites were shorter than the typically 10 μm-long wild-type sporozoites. Not surprisingly, PINA270 sporozoites were not infective. They did not infect mosquito salivary glands, as shown by the greatly reduced ratio of salivary gland to midgut sporozoites, and were also incapable of displaying the normal gliding phenotype (not shown).

The intermediate phenotype of PINA270 oocysts is due to the low amounts of CS produced

To demonstrate that the phenotypes displayed by the PINA270 clones were due to the low amounts of CS, we constructed a control parasite clone, PINA450, using a strategy similar to that used to construct the PINA270 clones but using an insertion plasmid (pPINA450) where the truncated *CS* was followed by 450 bp of 3′-UTR. This 3′-UTR was identical to that present in plasmid pCSComp, and included the GT-rich sequence located ~350 bp downstream of the stop codon (see Figure 7A). PINA450 clonal parasites were obtained that contained a single copy of plasmid PINA450 integrated at the *CS* locus (Figure 7B and E), in which expression of the full-length *CS* was therefore driven by 450 bp of 3′-UTR (Figure 7F).

Normal numbers of PINA450 sporozoites were produced in mosquito midguts (not shown). Western blot analysis showed that they produced amounts of CS similar to wild-type sporozoites (Figure 7G). Upon examination by immunofluorescence microscopy using anti-CS antibodies, PINA450 and wild-type sporozoites displayed undistinguishable average size and shape, i.e. >90% being the typical ~10 μm long, ~1 μm wide, crescent-shaped cells. Comparison of infective, invasive and gliding capacities of PINA450 and wild-type sporozoites showed that the former had regained a fully wild-type phenotype (not shown). These results demonstrate that the phenotype of PINA270 oocysts is due to the low amounts of CS produced, and not to an undesired effect of the PINA recombinant locus.

Discussion

Cell division in Apicomplexa protozoa, unlike in most other eukaryotes, is not coupled to DNA replication and nuclear division. In these parasites, multiple rounds of karyokinesis typically take place in the absence of cytokinesis, before uninucleate daughter cells bud along the plasma membrane of the syncytial mother cell (a process called schizogony). In *Plasmodium*, the oocyst generates thousands of sporozoites in a highly coordinated budding process, which occurs by successive waves (Vanderberg *et al*., 1967). Here, we provide evidence that establishment of polarity in the *Plasmodium* oocyst and sporozoite budding depend on the CS protein, mainly known as a sporozoite surface protein critical to sporozoite infectivity.

Ultrastructural studies in numerous apicomplexan genera have shown that budding is concomitant with microtubule polymerization. Recent drug inhibition studies in *Toxoplasma* have suggested further that microtubule, but not actin polymerization is essential for efficient budding (Shaw *et al*., 2000). What triggers budding, however, is unknown. In mother cells of most Apicomplexa, particularly those generating numerous daughter cells, nuclei migrate to the plasma membrane and frequently make contact via a membrane portion that contains a centrosome/spindle pole body associated with an intranuclear spindle (Terzakis *et al*., 1967; Vanderberg and Rhodin, 1967; Sinden and Strong, 1978; Shaw and Tilney, 1992). Thus an early event involved in daughter cell budding may be the positioning of a microtubule-organizing center (MTOC), which nucleates and orients microtubule assembly, at the plasma membrane of the mother cell. This could be achieved by a typical search–capture mechanism of MTOC attachment to cortical sites (Desai and Mitchison, 1997), whereby a microtubule captured by a binding site depolymerizes and drags the MTOC towards the site. This mechanism is widely used for generating asymmetric microtubule distribution, including for positioning the budding yeast spindle to the mother-bud neck (Carminati and Stearns, 1997; Kaverina *et al*., 1998; Addox *et al*., 1999).

Daughter cell formation follows the growth of the microtubule skeleton (D'Haese *et al*., 1977; Desser, 1980; Paterson and Desser, 1981; Shaw and Tilney, 1992; Shaw *et al*., 2001). Subpellicular microtubules radiate from the MTOC, known as the polar ring, and progressively surround the bound nucleus and the set of organelles attached to the nuclear membrane. As the microtubule skeleton is likely to grow inside the mother cell (fast-growing ends of microtubules typically are distal to the MTOC, including in the Apicomplexan *Eimeria*; Russell and Burns, 1984), a cell may be formed by progressively docking the plasma membrane around the internally growing skeleton. Alternatively, the inner membrane–microtubule lattice may be pushed out as it is formed, and daughter cells extruded from the mother cell surface. In *Plasmodium* oocysts, the dense collar of intramembranous particles that encircles the bases of sporozoite buds (Meszoely *et al*., 1989) may be involved in such a process, as well as in membrane incorporation in the forming cell.

The CS protein is first expressed by the young *Plasmodium* oocyst and is detected mainly at the plasma membrane (Nagasawa *et al*., 1987, 1988; Posthuma *et al*., 1988; Aikawa *et al*., 1990; this work). Here, we found an inverse correlation between the amounts of the CS protein produced by the parasite and the levels of extension of the inner membranes and microtubules underneath the oocyst plasma membrane. In the CSko clone, inner membranes and microtubules underlined the entire plasma membrane, and sporozoite morphogenesis was profoundly altered. In the PINA270 clone, which produces ~5× less CS than the wild-type, inner membranes and microtubules underlined extensive areas of the oocyst plasma membrane, and sporozoites were misshapen. In contrast, sporozoites were formed normally by the PINA450 and the complemented CSko clones, which both produced wild-type amounts of CS.

Various morphological lines of evidence suggest that CS plays a specific role in restricting assembly and/or elongation of the inner membranes and microtubules. Extensive development of these structures was the first recognizable effect of the lack of CS. It occurred early during development, as inner membranes and microtubules in the CSko clone emerged underneath local invaginations of a plasma membrane that was not yet fully retracted from the capsule, unlike in the wild type. Furthermore, low amounts or lack of CS always caused regular extension of inner membranes and microtubules underneath the plasma membrane, suggesting that productive docking events still occurred at the plasma membrane. Finally, expression of 5× less CS protein induced levels of extension that were intermediate between those of the CSko and wild-type parasites. These data suggest that CS is involved in a specific mechanism that inhibits premature assembly and/or incorrect elongation of the inner membranes and microtubules.

What causes the pathological extension of the microtubule skeleton and associated inner membranes in *CS* mutants? A first hypothesis is that subpellicular microtubules are free or nucleated at MTOCs that are not polar rings, i.e. that lack of CS activates ectopic microtubule nucleation/polymerization unrelated to normal budding. However, microtubules in *CS* mutants were always associated with the plasma membrane. In addition, the spacing between individual microtubules and the distance between microtubules and the inner membranes or the plasma membrane were strikingly similar in mutants and the wild type. This rather suggests that in *CS* mutants microtubules are also nucleated at polar rings, and that their polymerization follows a budding signal. Another hypothesis is that aberrant microtubule polymerization in *CS* mutants results from incorrect bud growth. However, lack of CS did not prevent co-elongation of inner membranes and microtubules, or the formation of sporozoite-like buds that normally segregated nuclei and rhoptries. Also, the effects of the *CS* mutations occurred before budding started in the wild type (at the stage of subcapsular vacuolization), arguing against a role for CS in simply shaping the bud. A more likely hypothesis would be that CS is involved in preventing premature budding initiation. In this case, membrane-associated CS would restrict formation of or accessibility to a budding cue, or its recognition by a docking partner. The aberrant shapes of buds in CSko oocysts would result from the premature or

incorrect assembly of the budding site, possibly via altered positioning of the MTOC at the plasma membrane.

The nature of the sporozoite budding cue in *Plasmodium* oocysts is unknown, but probably includes some cortical component. In model cell types, polarity is established by a cascade of molecular events initiated by a spatial cue at the cell surface. In the budding yeast, the budding site is established via an intrinsic cue, which is composed of actin and septins and demarcated by the budding site of the previous cell cycle (Chant, 1999; Pruyne and Bretscher, 2000a,b). In epithelial cells, polarity arises from extrinsic cues, i.e. extracellular ligands binding to adhesion receptors, cadherins and integrins, which in turn recruit cytoskeletal proteins (Drubin and Nelson, 1996). In the *Plasmodium* oocyst, budding sites are unlikely to be defined by inherited spatial landmarks from the previous division cycle, or by ligands in the subcapsular space. A simple hypothesis is that budding cues are present randomly at the plasma membrane, and are regulated negatively by CS. As CS appears to be GPI anchored (Moran and Caras, 1994), its diffusion in membrane microdomains and the dynamic nature of rafts may play a role in regulating access to budding cues, via transient formation of plasma membrane areas where CS is absent or inactive. Varying the levels of a budding inhibitor may provide a simple way of creating budding sites in a syncitium that needs to partition thousands of cells in successive waves, ultimately to achieve organized cell division.

The CS protein of *Plasmodium* has evolved to carry out numerous functions during the parasite life cycle. On the surface of sporozoites, CS plays various roles in sporozoite pathogenicity, including in adhesion to mosquito salivary glands and mammalian hepatocytes, and probably also in gliding motility, a process key for host cell invasion (Stewart and Vanderbeg, 1988; Cerami *et al*., 1992; Warburg *et al*., 1992). CS carried in mammalian cells by invading sporozoites may also inhibit protein synthesis in the host cell (Frevert *et al*., 1998). We have shown that CS is essential for sporozoite budding inside oocysts, by organizing formation of the sporozoite cytoskeleton. CS thus controls all aspects of the sporozoite life, from birth to development into the next stage. The genetic link between formation and infectivity of the sporozoite may help to generate only sporozoites that are maximally fit for their adventurous journey.

Materials and methods

Parasites

The following clones of *P.berghei* were used in this study: a wild-type pyrimethamine-sensitive, gametocyte-producing clone of the NK65 strain (Ménard *et al*., 1997), and the pyrimethamine-resistant CS knockout clone CS(-)1 (CSko) that contains a single copy of the pyrimethamine-resistant *P.berghei DHFR-TS* gene inserted into the open reading frame (ORF) of the single-copy *CS* gene (Ménard *et al*., 1997).

Construction of targeting plasmid pCSComp containing the human DHFR gene

Plasmid pCSComp (Figure 6A), used for the complementation of CSko parasites, contains the h*DHFR* gene flanked by 2.2 and 0.55 kb of 5′- and 3′-UTRs of *P.berghei DHFR-TS*, respectively (de Koning-Ward *et al*., 2000), and a targeting sequence consisting of a wild-type *CS* expression cassette. Plasmid pCSComp was constructed by inserting the fragment of *CS* isolated from *P.berghei* strain NK65 (Eichinger *et al*., 1986) bearing the full ORF (~1 kb), and 1.3 and 0.45 kb of flanking *CS* 5′- and 3′-UTRs, respectively, digested with *Pst*I (New England Biolabs), filled in and digested with *Eco*RI, into plasmid pDb.Dh. Db (de Koning-Ward *et al*., 2000) containing the h*DHFR* selection cassette cut with *Kpn*I, filled in and digested with *Eco*RI. To promote homologous integration of pCSComp upstream of the disrupted *CS* locus in CSko parasites (Nunes *et al*., 1999), ~50 μg of the plasmid was linearized at the unique *Kpn*I site located ~600 bp upstream of the *CS* start codon.

Construction of plasmids pPINA270 and pPINA450

The insertion plasmid pPINA270 (Figure 7A) contains the pyrimethamine-resistant *P.berghei DHFR-TS* gene expressed by its own 5′- (2.2 kb) and 3′- (0.4 kb) UTRs, and a targeting sequence (~1.2 kb) consisting of the distal part of *CS*, lacking the first 11 codons, and followed by 0.27 kb of downstream UTR. A unique *Afl*II site was introduced by PCR ~250 bp from the 5′ end of the *CS* targeting sequence using the following oligonucleotides: BamS12 (sense, 5′-gcgggatccctttattagttaattctctacttccagga-3′, *Bam*HI site underlined), AflIIA (antisense, 5′-gcgcttaagtttattattacgctctatttttcgt-3′, *Afl*II site underlined), AflIIB (sense, 5′-gcgcttaagcaaccaccaccaccaccaaac-3′, *Afl*II site underlined) and NotA (antisense, 5′-gcggcggccgctacatatataataaacacgaaaaaaataaacta-3′, *Not*I site underlined). Plasmid pPINA450 (Figure 7A) is identical to plasmid pPINA270 except that it contains 0.45 kb of *CS* 3′ UTR, which was cloned by PCR from *P.berghei* strain NK65 genomic DNA using the following primers: POSBAM (sense, 5′-gcgggatcccaaggttcaaataagaaagca-3′, *Bam*HI site underlined), which hybridized from nucleotide 878 of *CS* onwards, and PYCS3UTR (antisense, 5′-atttgcggccgccacaaaataaataatttggatagctacataaaatg-3′, *Not*I site underlined). The antisense primer was based on a published sequence of *CS* 3′-UTR from *P.yoelii*, a related rodent *Plasmodium* species (Lal *et al*., 1987). The PCR product was subcloned into a pPCR-Script Amp SK(+) cloning vector (Stratagene) and used to replace its counterpart in plasmid pPINA270. To obtain efficient homologous integration of the insertion plasmids at the *CS* locus, ~50 μg of pPINA270 or pPINA450 were linearized within the region of homology at the PCR-generated *Afl*II site prior to transfection (Nunes *et al*., 1999). The *Afl*II site present in these targeting plasmids is not retained after plasmid integration at the *CS* locus.

Parasite transfection and selection of recombinants

Plasmodium berghei schizonts (~1×10^8) were prepared for transfection, and targeting plasmids were introduced by electroporation as previously described (Ménard and Janse, 1997; Waters *et al*., 1997). For gene targeting experiments in the CSko clone of *P.berghei* using the h*DHFR* selectable marker and WR99210 selection, four recipient rats were treated for three consecutive days with a single intraperitoneal dose of WR99210 (5 mg/kg of body weight), starting 27–30 h after injection of the electroporated parasites. WR99210 was provided by David Jacobus (Jacobus Pharmaceuticals) and prepared fresh as a 5 mg/ml solution in phosphate-buffered saline (PBS) containing 10% dimethylsulfoxide.

Southern hybridization and PCR analysis of resistant parasite populations

Southern blotting was performed using either of the following probes: a *CS* probe (0.7 kb *Hin*cII–*Xmn*I internal fragment of the coding sequence), a *P.berghei DHFR-TS* probe (1.2 kb *Xba*I–*Hin*dIII internal fragment) or a h*DHFR* probe (0.56 kb encompassing the entire coding sequence). Probes were labeled with digoxigenin (DIG)-ddUTP by random priming, and the chemiluminescence was detected using CSPD (Roche Molecular Biochemicals). Specific amplification of the first duplicate of a recombinant locus obtained after integration of plasmid pPINA270 or pPINA450 was performed with primers O1CS (sense, 5′-atgaagaagtgtaccattttagttgtagcg-3′, which hybridizes to the first 10 codons of *CS* that are absent in the targeting plasmids) and primer T7 (antisense, 5′-gtaatacgactcactatagggc-3′, which hybridizes to the bacterial plasmid pBSKS).

Analysis of parasite development and infectivity

Anopheles stephensi mosquitos were fed on infected young Sprague–Dawley rats and dissected at various days post-infection. Sporozoite populations were prepared from the various mosquito compartments and analyzed as previously described (Vanderberg, 1975; Sultan *et al*., 1997).

Indirect immunofluorescence assays

Plasmodium berghei hemolymph or salivary gland sporozoites were collected at days 15–18 post-feeding, air-dried on glass slides and fixed with 2% paraformaldehyde for 30 min at room temperature. Sporozoites

were then pre-incubated in PBS–3% bovine serum albumin (BSA) for 30 min at room temperature followed by incubation with fluorescein isothiocyanate (FITC)-conjugated anti-CS monoclonal antibody 3D11 (Yoshida *et al*., 1980) for 1 h at 37°C in a humidified chamber. After three washes in PBS, sporozoites were mounted in Vectashield (Vector Laboratories) and visualized using a Nikon inverted epifluorescence microscope equipped with a 60× objective (Figure 6D), or a Zeiss fluorescent microscope equipped with a 63×/1.40 oil immersion objective (Figure 8).

Western analysis of sporozoite lysates

The *P.berghei* midgut sporozoites were collected in RPMI medium containing the Complete™ Mini protease inhibitor cocktail (Roche Molecular Biochemicals) from oocysts developing in *A.stephensi* midguts between days 13 and 15 post-infection, and counted using a hemocytometer. Crude extracts were prepared in SDS sample buffer. Protein samples from defined numbers of sporozoites were loaded per lane in SDS sample buffer containing 10% β-mercaptoethanol, resolved on 10% SDS–polyacrylamide gels (Laemmli, 1970) and transferred to 0.2 μm PVDF membranes (Bio-Rad) by electrophoretic transfer. The membranes were incubated overnight in blocking buffer at 4°C and then probed with anti-CS monoclonal antibody 3D11, diluted 1:5000 in blocking buffer, for 1 h at room temperature. The membranes were washed three times in wash buffer and incubated for 1 h with horseradish peroxidase (HRP)-conjugated goat anti-mouse IgG (Promega), diluted 1:20 000 in blocking buffer. The membranes were washed, and bound antibodies were visualized using the enhanced chemiluminescence (ECL) system (Amersham) according to the manufacturer's instructions. The same blot was rinsed with water and then reprobed with anti-TRAP polyclonal antibodies diluted 1:2000 in blocking buffer, followed by incubation with HRP-conjugated goat anti-rabbit IgG diluted 1:20 000 in blocking buffer. Bound antibodies were visualized using ECL.

Transmission electron microscopy

Plasmodium berghei (wild-type, CSko and PINA270 clones) oocysts within mosquito midguts were fixed with 2.5% glutaraldehyde in 0.05 M phosphate buffer pH 7.4 with 4% sucrose for 2 h and then post-fixed in 1% osmium tetroxide for 1 h. After a 30 min *en bloc* stain with 1% aqueous uranyl acetate, the cells were dehydrated in ascending concentrations of ethanol and embedded in Epon 812. Ultrathin sections were stained with 2% uranyl acetate in 50% methanol and with lead citrate, and then examined in a Zeiss CEM902 electron microscope.

Immunoelectron microscopy

Plasmodium berghei (wild-type and PINA270 lines) oocysts within mosquito midguts were fixed with 1% formaldehyde, 0.5% glutaraldehyde in 0.1 M phosphate buffer pH 7.4. Fixed samples were washed, dehydrated and embedded in LR White resin (Polysciences, Inc., Warrington, PA) as described previously described (Aikawa *et al*., 1990). Thin sections were blocked in PBS containing 0.01% (v/v) Tween-20 and 5% (w/v) non-fat dry milk (PBTM). Grids were then incubated for 2 h at room temperature with the primary mouse anti-CS monoclonal antibody 3D11, diluted 1:500 in PBTM. Normal mouse serum or PBTM were used as negative controls. After washing, grids were incubated for 1 h with 15 nm gold-conjugated goat anti-mouse IgG (Amersham Life Sciences), diluted 1:20 in PBS containing 1% (w/v) BSA and 0.01% (v/v) Tween-20, rinsed with Tween-20, and fixed with glutaraldehyde to stabilize the gold particles. Samples were stained with uranyl acetate and lead citrate, and then examined in a Zeiss CEM902 electron microscope.

Scanning electron microscopy

Free midgut sporozoites were fixed with 2.5% glutaraldehyde in 0.05 M phosphate buffer pH 7.4 with 4% sucrose for 2 h and then post-fixed in 1% osmium tetroxide for 1 h. Samples were dehydrated in graded ethanol, critical-point dried (Balzers CPD020 critical-point dryer) and mounted on a coverslip. Samples were coated with gold in an RMC-Eiko RE sputter coater, and then examined in a JEOL JSM-840 scanning electron microscope.

Acknowledgements

We thank Freddy Frischknecht, Jayne Raper, Photini Sinnis, Régis Tournebize and Jerome Vanderberg for reviewing the manuscript, and Jean-François Dubremetz and David Roos for many helpful discussions.

References

Addox,P., Chin,E., Mallavarapu,A., Yeh,E., Salmon,E.D. and Bloom,K. (1999) Microtubule dynamics from mating through the first zygotic division in the budding yeast *Saccharomyces cerevisiae*. *J. Cell Biol.*, **144**, 977–987.

Aikawa,M. (1971) *Plasmodium*: the fine structure of malaria parasites. *Exp. Parasitol.*, **30**, 284–320.

Aikawa,M. (1988) Fine structure of malaria parasites in the various stages of development. In Wernsdorfer,W.H. and McGregor,I. (eds), *Malaria: Principles and Practice of Malariology*. Churchill Livingstone, New York, NY, Vol. 1, pp. 97–129.

Aikawa,M., Yoshida,N., Nussenzweig,R.S. and Nussenzweig,V. (1981) The protective antigen of malarial sporozoites (*Plasmodium berghei*) is a differentiation antigen. *J. Immunol.*, **126**, 2494–2495.

Aikawa,M., Atkinson,C.T., Beaudoin,L.M., Sedegah,M., Charoenvit,Y. and Beaudoin,R. (1990) Localization of CS and non-CS antigens in the sporogonic stages of *Plasmodium yoelii*. *Bull. World Health Organ.*, **68**, 165–171.

Carminati,J.L. and Stearns,T. (1997) Microtubules orient the mitotic spindle in yeast through dynein-dependent interactions with the cell cortex. *J. Cell Biol.*, **138**, 629–641.

Cerami,C., Frevert,U., Sinnis,P., Takacs,B., Clavijo,P., Santos,M.J. and Nussenzweig,V. (1992) The basolateral domain of the hepatocyte plasma membrane bears receptors for the circumsporozoite protein of *Plasmodium falciparum* sporozoites. *Cell*, **70**, 1021–1033.

Chant,J. (1999) Cell polarity in yeast. *Annu. Rev. Cell. Dev. Biol.*, **15**, 365–391.

deKoning-Ward,T.F., Fidock,D.A., Thathy,V., Ménard,R., van Spaendonk,R.M., Waters,A.P. and Janse,C.J. (2000) The selectable marker human dihydrofolate reductase enables sequential genetic manipulation of the *Plasmodium berghei* genome. *Mol. Biochem. Parasitol.*, **106**, 199–212.

deLaraCapurro,M., Coleman,J., Beerntsen,B.T., Myles,K.M., Olson, K.E., Rocha,E., Krettli,A.U. and James,A.A. (2000) Virus-expressed, recombinant single-chain antibody blocks sporozoite infection of salivary glands in *Plasmodium gallinaceum*-infected *Aedes aegypti*. *Am. J. Trop. Med. Hyg.*, **62**, 427–433.

Desai,A. and Mitchison,T.J. (1997) Microtubule polymerization dynamics. *Annu. Rev. Cell. Dev. Biol.*, **13**, 83–117.

Desser,S.S. (1980) An utltrastructural study of the asexual development of a presumed *Isospora* sp. in mononuclear phagocytic cells of the evening grosbeak (*Hesperiphora vespertia*). *J. Parasitol.*, **66**, 601–612.

D'Haese,J., Mehlhorn,H. and Peters,W. (1977) Comparative study of pellicular structures in coccidia. *Int. J. Parasitol.*, **7**, 505–518.

Drubin,D.G. and Nelson,W.J. (1996) Origins of cell polarity. *Cell*, **84**, 335–344.

Dubremetz,J.F. and Torpier,G. (1978) Freeze fracture study of the pellicle of an eimerian sporozoite (Protozoa, Coccidia). *J. Ultrastruct. Res.*, **62**, 94–109.

Eichinger,D.J., Arnot,D.E., Tam,J.P., Nussenzweig,V. and Enea,V. (1986) Circumsporozoite protein of *Plasmodium berghei*: gene cloning and identification of the immunodominant epitopes. *Mol. Cell. Biol.*, **6**, 3965–3972.

Fidock,D.A. and Wellems,T.E. (1997) Transformation with human dihydrofolate reductase renders malaria parasites insensitive to WR99210 but does not affect the intrinsic activity of proguanil. *Proc. Natl Acad. Sci. USA*, **94**, 10931–10936.

Frevert,U., Sinnis,P., Cerami,C., Shreffler,W., Takacs,B. and Nussenzweig,V. (1993) Malaria circumsporozoite protein binds to heparan sulfate proteoglycans associated with the surface membrane of hepatocytes. *J. Exp. Med.*, **177**, 1287–1298.

Frevert,U., Galinski,M.R., Hugel,F.U., Allon,N., Schreier,H., Smulevitch,S., Shakibaei,M. and Clavijo,P. (1998) Malaria circumsporozoite protein inhibits protein synthesis in mammalian cells. *EMBO J.*, **17**, 3816–3826.

Gantt,S.M., Clavijo,P., Bai,X., Esko,J.D. and Sinnis,P. (1997) Cell adhesion to a motif shared by the malaria circumsporozoite protein and thrombospondin is mediated by its glycosaminoglycan-binding region and not by CSVTCG. *J. Biol. Chem.*, **272**, 19205–19213.

Kaverina,I., Rottner,K. and Small,J.V. (1998) Targeting, capture and stabilization of microtubules at early focal adhesions. *J. Cell Biol.*, **142**, 181–190.

Laemmli,U.K. (1970) Cleavage of structural proteins during the assembly of the head of bacteriophage T4. *Nature*, **227**, 680–685.

Lal,A.A., de la Cruz,V.F., Welsh,J.A., Charoenvit,Y., Maloy,W.L. and

McCutchan,T.F. (1987) Structure of the gene encoding the circumsporozoite protein of *Plasmodium yoelii*. A rodent model for examining antimalarial sporozoite vaccines. *J. Biol. Chem.*, **262**, 2937–2940.

Ménard,R. and Janse,C.J. (1997) Gene targeting in malaria parasites. *Methods*, **13**, 148–157.

Ménard,R., Sultan,A.A., Cortes,C., Altszuler,R., van Dijk,M.R., Janse, C.J., Waters,A.P., Nussenzweig,R.S. and Nussenzweig,V. (1997) Circumsporozoite protein is required for development of malaria sporozoites in mosquitoes. *Nature*, **385**, 336–340.

Meszoely,C.A.M., Erbe,E.F., Beaudoin,L.M. and Beaudoin,R.L. (1989) Freeze-fracture studies on the sporoblast and sporozoite development in the early oocyst. *Am. J. Trop. Med. Hyg.*, **41**, 499–503.

Moran,P. and Caras,I.W. (1994) Requirements for glycosylphosphatidylinositol attachment are similar but not identical in mammalian cells and parasitic protozoa. *J. Cell Biol.*, **125**, 333–343.

Morrissette,N.S., Murray,J.M. and Roos,D.S. (1997) Subpellicular microtubules associate with an intramembranous particle lattice in the protozoan parasite *Toxoplasma gondii*. *J. Cell Sci.*, **110**, 35–42.

Nagasawa,H., Procell,P.M., Atkinson,C.T., Campbell,G.H., Collins,W.E. and Aikawa,M. (1987) Localization of circumsporozoite protein of *Plasmodium ovale* in midgut oocysts. *Infect. Immun.*, **55**, 2928–2932.

Nagasawa,H., Aikawa,M., Procell,P.M., Campbell,G.H., Collins,W.E. and Campbell,C.C. (1988) *Plasmodium malariae*: distribution of circumsporozoite protein in midgut oocysts and salivary gland sporozoites. *Exp. Parasitol.*, **66**, 27–34.

Nunes,A., Thathy,V., Bruderer,T., Sultan,A.A., Nussenzweig,R.S. and Ménard,R. (1999) Subtle mutagenesis by ends-in recombination in malaria parasites. *Mol. Cell. Biol.*, **19**, 2895–2902.

Pancake,S.J., Holt,G.D., Mellouk,S. and Hoffman,S.L. (1992) Malaria sporozoites and circumsporozoite proteins bind specifically to sulfated glycoconjugates. *J. Cell Biol.*, **117**, 1351–1357.

Paterson,W.B. and Desser,S.S. (1981) An utrastructural study of *Eimeria iroquoina* in experimentally infected fathead minnows. *J. Protozool.*, **28**, 302–308.

Pinzon-Ortiz,C., Friedman,J., Esko,J. and Sinnis,P. (2001) The binding of the circumsporozoite protein to cell surface proteoglycans is required for *Plasmodium* sporozoite attachment to target cells. *J. Biol. Chem.*, **276**, 26784–26791.

Posthuma,G., Meis,J.F., Verhave,J.P., Hollingdale,M.R., Ponnudurai,T., Meuwissen,J.H. and Geuze,H.J. (1988) Immunogold localization of circumsporozoite protein of the malaria parasite *Plasmodium falciparum* during sporogony in *Anopheles stephensi* midguts. *Eur. J. Cell Biol.*, **46**, 18–24.

Pruyne,D. and Bretscher,A. (2000a) Polarization of cell growth in yeast. I. Establishment and maintenance of polarity states. *J. Cell Sci.*, **113**, 365–375.

Pruyne,D. and Bretscher,A. (2000b) Polarization of cell growth in yeast. II. The role of the cortical actin cytoskeleton. *J. Cell Sci.*, **113**, 571–585.

Russell,D.G. and Burns,R.G. (1984) The polar ring of coccidian sporozoites: a unique microtubule-organizing centre. *J. Cell Sci.*, **65**, 193–207.

Ruvolo,V., Altszuler,R. and Levitt,A. (1993) The transcript encoding the circumsporozoite antigen of *Plasmodium berghei* utilizes heterogeneous polyadenylation sites. *Mol. Biochem. Parasitol.*, **57**, 137–150.

Shaw,M.K. and Tilney,L.G. (1992) How individual cells develop from a syncytium: merogony in *Theileria parva* (Apicomplexa). *J. Cell Sci.*, **101**, 109–123.

Shaw,M.K., Compton,H.L., Roos,D.S. and Tilney,L.G. (2000) Microtubules, but not actin filaments, drive daughter cell budding and cell division in *Toxoplasma gondii*. *J. Cell Sci.*, **113**, 1241–1254.

Shaw,M.K., Roos,D.S. and Tilney,L.G. (2001) DNA replication and daughter cell budding are not tightly linked in the protozoan parasite *Toxoplasma gondii*. *Microbes Infect.*, **3**, 351–362.

Sidjanski,S.P., Vanderberg,J.P. and Sinnis,P. (1997) *Anopheles stephensi* salivary glands bear receptors for region I of the circumsporozoite protein of *Plasmodium falciparum*. *Mol. Biochem. Parasitol.*, **90**, 33–41.

Sinden,R. (1978) Cell biology. In Jones,R.K. (ed.), *Rodent Malaria*. Academic Press, New York, NY, pp. 85–168.

Sinden,R.E. and Strong,K. (1978) An ultrastructural study of the sporogonic development of *Plasmodium falciparum* in *Anopheles gambiae*. *Trans. R. Soc. Trop. Med. Hyg.*, **72**, 477–491.

Sinnis,P., Clavijo,P., Fenyo,D., Chait,B.T., Cerami,C. and Nussenzweig,V. (1994) Structural and functional properties of region II-plus of the malaria circumsporozoite protein. *J. Exp. Med.*, **180**, 297–306.

Sinnis,P., Willnow,T.E., Briones,M.R., Herz,J. and Nussenzweig,V. (1996) Remnant lipoproteins inhibit malaria sporozoite invasion of hepatocytes. *J. Exp. Med.*, **184**, 945–954.

Stewart,M.J. and Vanderberg,J.P. (1988) Malaria sporozoites leave behind trails of circumsporozoite protein during gliding motility. *J. Protozool.*, **35**, 389–393.

Sultan,A.A., Thathy,V., Frevert,U., Robson,K.J., Crisanti,A., Nussenzweig,V., Nussenzweig,R.S. and Ménard,R. (1997) TRAP is necessary for gliding motility and infectivity of *Plasmodium* sporozoites. *Cell*, **90**, 511–522.

Terzakis,J.A., Sprinz,H. and Ward,R.A. (1967) The transformation of the *Plasmodium gallinaceum* oocyst in *Aedes aegypti* mosquitoes. *J. Cell Biol.*, **34**, 311–326.

Vanderberg,J.P. (1975) Development of infectivity by the *Plasmodium berghei* sporozoite. *J. Parasitol.*, **61**, 43–50.

Vanderberg,J. and Rhodin,J. (1967) Differentiation of nuclear and cytoplasmic fine structure during sporogonic development of *Plasmodium berghei*. *J. Cell Biol.*, **32**, C7–C10.

Vanderberg,J., Rhodin,J. and Yoeli,M. (1967) Electron microscopic and histochemical studies of sporozoite formation in *Plasmodium berghei*. *J. Protozool.*, **14**, 82–103.

Warburg,A., Touray,M., Krettli,A.U. and Miller,L.H. (1992) *Plasmodium gallinaceum*: antibodies to circumsporozoite protein prevent sporozoites from invading the salivary glands of *Aedes aegypti*. *Exp. Parasitol.*, **75**, 303–307.

Waters,A.P., Thomas,A.W., van Dijk,M.R. and Janse,C.J. (1997) Transfection of malaria parasites. *Methods*, **13**, 134–147.

Yoshida,N., Nussenzweig,R.S., Potocnjak,P., Nussenzweig,V. and Aikawa,M. (1980) Hybridoma produces protective antibodies directed against the sporozoite stage of malaria parasite. *Science*, **207**, 71–73.

Yoshida,N., Potocnjak,P., Nussenzweig,V. and Nussenzweig,R.S. (1981) Biosynthesis of Pb44, the protective antigen of sporozoites of *Plasmodium berghei*. *J. Exp. Med.*, **154**, 1225–1236.

Received January 10, 2002; revised and accepted February 14, 2002